A&A manuscript no.
(will be inserted by hand later)

Your thesaurus codes are:
08(08.06.2;08.06.3;08.12.2;08.12.3;08.16.5;13.09.6)

ASTRONOMY AND ASTROPHYSICS
September 6, 1999

ISOCAM observations of the RCrA star formation region ⋆

G. Olofsson[1], **M. Huldtgren**[1], **A.A. Kaas**[1], **S. Bontemps**[1,2], **L. Nordh**[1], **A. Abergel**[3], **P. André**[4], **F. Boulanger**[3], **M. Burgdorf**[5], **M.M. Casali**[6], **C.J Cesarsky**[4], **J. Davies**[10], **E. Falgarone**[7], **T. Montmerle**[4], **M. Perault**[7], **P. Persi**[8], **T. Prusti**[5], **J.L. Puget**[3], and **F. Sibille**[9]

[1] Stockholm Observatory, SE–133 36 Saltsjöbaden, Sweden
[2] Observatoire de Bordeaux, Floirac, France
[3] IAS, Université Paris XI, Orsay, France
[4] Service d'Astrophysique, CEA Saclay, Gif-sur-Yvette, France
[5] ISO Data Centre, ESA Astrophysics Division, Villafranca del Castillo, Spain
[6] Royal Observatory, Blackford Hill, Edinburgh, UK
[7] ENS Radioastronomie, Paris, France
[8] IAS, CNR, Rome, Italy
[9] Observatoire de Lyon, France
[10] Joint Astronomy Center, Hawaii

Received ; Accepted

Abstract. The results of an ISOCAM survey of the RCrA star formation region are presented. The survey was carried out in two broad-band filters, LW2 (5–8.5 μm) and LW3 (12–18 μm). Although it was not possible to map the densest, central region due to saturation problems, 21 sources were identified which showed mid-IR excesses. Most of these sources have not previously been recognised as YSOs (Young Stellar Objects), mainly because they are relatively faint. We find evidence for a population of very low mass stars which are probably brown dwarfs in their early contraction phases.

Key words: stars: formation – stars: fundamental parameters – stars: low-mass, brown dwarfs – stars: luminosity function, mass function – stars: pre-main sequence – infrared: stars

1. Introduction

The nearest star formation regions have been surveyed in an ISOCAM programme (Nordh et al. 1998), and in this paper we present the results for the RCrA region. This bow-shaped, dense molecular cloud core has a mass of about 120 $M_\odot$ (Harju et al. 1993) and hosts a region of vigorous star formation activity with the usual indicators: a group of bright, pre-main-sequence (PMS) stars (Graham 1991); a bipolar outflow (Andersson et al. 1997); compact HII regions (Brown 1987) and Herbig-Haro objects (Hartigan & Graham 1987). The distance to the cloud has been determined by Marraco & Rydgren (1981) as 129 pc. Since the region also is located far away from the Galactic plane (b=–18°), it provides a favourable target for detailed studies. The young stellar population has been studied using several techniques to identify the members: Hα surveys (Marraco & Rydgren 1981), optical spectroscopy (Walter et al. 1997), near and far IR mapping (e.g. Wilking et al. 1992 and Wilking et al. 1997) and X-ray mapping (Patten 1998). Altogether these investigations have identified approximately 40 members believed to represent the young stellar population.

Due to the high sensitivity and high spatial resolution, ISOCAM offered an unique possibility to identify young stars with mid-IR excesses. The advantage of mid-IR observations in searching for YSOs is not immediately clear and we have to consider the following questions:

1. Do YSOs in general exhibit mid-IR excesses?
2. Is it possible to separate reddened background sources from the YSOs?
3. Are other sources with mid-IR excesses, like evolved stars and IR galaxies, common enough to contaminate the sample of proposed YSOs?

These questions will be discussed below, but basically the prospects are favourable for a mid-IR YSO search: YSOs – if young enough – generally exhibit mid-IR excesses which can be observationally separated from the effects of interstellar reddening. In addition, for the sensitivity limit of the present ISOCAM observations, those background sources with similar mid-IR SEDs

Send offprint requests to: G. Olofsson

⋆ ISO is an ESA project with instruments funded by ESA Member States (especially the PI countries: France, Germany, the Netherlands and the United Kingdom) and with the participation of ISAS and NASA.

Correspondence to: olofsson@astro.su.se

(Spectral Energy Distributions) are rare. The preliminary results for the ISOCAM survey of the Chamaeleon and Ophiuchus regions (Nordh et al. 1996, Bontemps et al. 1998) clearly demonstrate the efficiency of sensitive mid-IR observations in identifying YSOs.

It is of particular interest to identify low luminosity YSOs as a way to study the mass distribution, the IMF (Initial Mass Function), for stars lying below the hydrogen burning limit (0.08 $M_{\odot}$). These stars gradually cool and fade away, but during their earliest contraction phases they are comparably bright and can be observed at the distances of the closest star formation regions. Even though such stars can be easily detected in the near-IR with modern array cameras, there are two reasons which make it difficult to judge if they are YSOs: cloud extinction often prevents their detection in the J filter (detection in three filters, usually J, H and K are required to separate intrinsic IR excess from interstellar reddening), and even if detections at these three wavelengths are at hand, the source of the excess emission is often too cool to be noticed in the near-IR, and observations at longer wavelengths are required (cf. Kenyon & Hartmann 1995). Another method used to identify YSO candidates in dark clouds is to study their variability, assuming that also the low-mass contracting stars exhibit light variations. This method has recently been found to be relatively efficient in the case of the Serpens region (Kaas 1999). Sensitive mapping in the mid-IR is, however, probably the most efficient method, and the ISO mission offered an excellent opportunity to conduct such observations. In this paper we report the results for the RCrA star formation region.

2. Observations and data reductions

Two regions, one to the west and the other to the east of the bright T Tauri star RCrA, were mapped with ISOCAM in the LW2 (5–8.5 μm) and LW3 (12–18 μm) filters using the image scale 6″/pixel. The unit integration time was 0.28 s and four such exposures were co-added onboard ISO for each transmitted frame. Around 18 frames were taken on each raster position. The raster orientation was in equatorial coordinates, and the overlap was one third of a frame in one direction and a few pixels in the other. The array had one dead column, and due to an unfortunate combination of spacecraft roll angle and raster parameters, this dead column remained uncovered, and 'dead stripes' remain in parts of the maps. These 'dead' areas correspond to three percent of the mapped regions and some faint stars could obviously escape detection for this reason. In addition, for stars detected in adjacent columns, the photometry is unreliable and therefore some 7% of the detected stars (including those close to the outer border of each map) lack reliable photometry. For the data reduction we used the CIA package (Ott et al. 1997) which included removal of glitches, dark subtraction, transient correction (using the IAS inversion method version 1.0, see Starck et al. 1999), flat fielding (using the zodiacal background) and projection of the frames into raster maps. The point sources were identified in the raster maps and traced back to the original frames for verification (to remove artefacts such as memory effects and glitch residuals) and photometry. The point spread function was used to correct the aperture photometry for the remaining flux outside the aperture.
The complete list of detected sources contains 234 objects of which 93% have photometry in LW2 and 21% in LW3. All of the sources detected in LW3 were also detected in LW2. This means, as indicated above, that 7% of the detected sources are located too close to the dead column or to the array border to allow photometry. We adopted the pre-launch conversion factors 1 mJy = 2.191 ADU/gain/s for LW2 and 1 mJy = 1.964 ADU/gain/s for LW3 (assuming a source with $F_{\lambda} \propto \lambda^{-1}$). These numbers will be modified as a result of the on-going ISOCAM calibration efforts, but the corrections are believed to be small. As regards the photometric accuracy we have considered the background definition and the source measure separately: For the background accuracy we use the co-added frame per raster position and calculate the spatial variation in the reference ring around the source. For the source accuracy we calculate the scatter of the measured flux within the aperture for each of the (typically) 18 frames. It turns out that these two parts are on the average equal. One would expect the background accuracy to be better determined as it represents a larger number of pixels, but residuals from glitches and non-cancelled transients from sources tend to increase the spatial noise. Obviously the presence of nebulosity also complicates the background definition. The median values for the point source accuracies ($1\,\sigma$) are 1.3 mJy for LW2 and 2.3 mJy for LW3, which also approximately represent the detection limits. For sources brighter than about $20\,\sigma$ the photometric accuracy is about 5% (excluding the uncertainty in the absolute calibration). It is of interest to compare the achieved sensitivity to the ultimate limit ($1\,\sigma$) as determined by the read-out noise, assuming no glitches, no memory effects and no nebulosity: for LW2 it would be 0.5 mJy and for LW3 0.7 mJy. We conclude that even though significant improvements as to the cosmetics of the final raster images can be achieved by e.g. correction for the optical distortion and by using a better transient correction, only marginal sensitivity improvements for point sources could be expected.

The positional accuracy was determined to be 0.3 s in right ascension and 2.5″ in declination ($1\,\sigma$) by using the 52 GSC (Guide Star Catalogue) stars detected in LW2. For consistancy, we list the ISO coordinates for all the sources (also for the sources with GSC and other optical

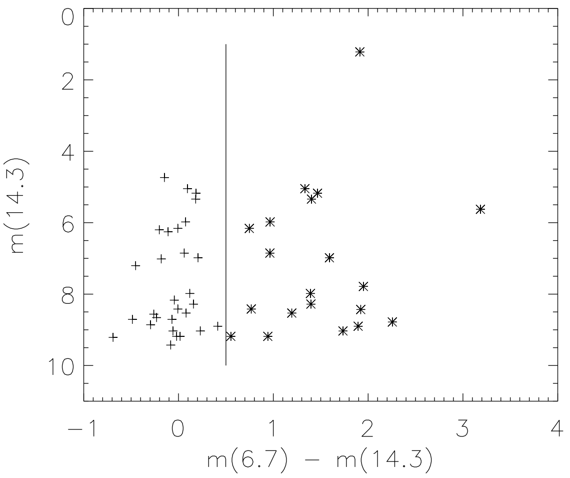

Fig. 2. In this colour/magnitude plot, two populations can be identified: one whose colour index is close to zero (as expected for normal stars) and another 'red' population. The symbols are the same as in Fig. 1

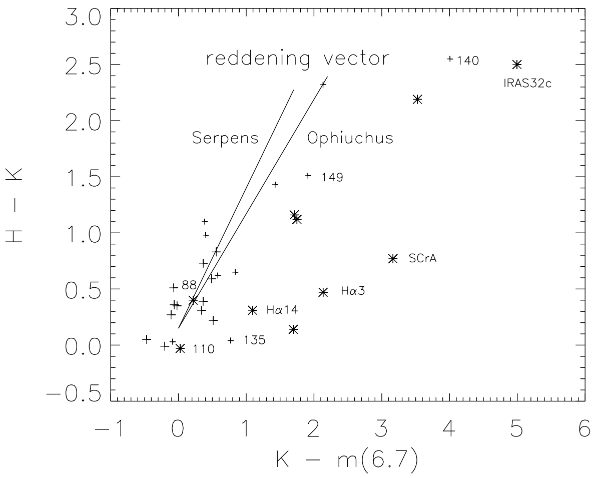

Fig. 3. In this colour/colour diagram for ISOCAM sources with published near-IR observation it is clear that sources that are 'red' in the $m_{6.7}$–$m_{14.3}$ index (asterisks) in general are 'red' also in the K–$m_{6.7}$ index. The symbols are the same as in Fig. 1. The two reddening lines represent preliminary results from our ISOCAM observations of the Serpens and Ophiuchus regions. At least two sources, ISO-CrA-135 and 140, which lack detection at 14.3 μm, have intrinsic K–$m_{6.7}$ excesses.

counterparts).

To conform to the magnitude system we adopt the following conversion: m(LW2) = $m_{6.7}$ = 0 for $1.81\,10^5$ ADU/gain/s and m(LW3) = $m_{14.3}$ = 0 for $3.71\,10^4$ ADU/gain/s. As for the conversion factors to mJy, it is expected that fine-tuning of this magnitude conversion will occur as a result of further calibration work.

In the following we will only discuss YSO candidates, but the full list of identified ISOCAM sources are available upon request (olofsson@astro.su.se). It should be stressed that due to the difficulties desrcibed above, sources brighter than the median $3\,\sigma$ (3.9 mJy and 6.9 mJy for the two filters respectively) may have been unnoticed. On the other hand we can with reasonable confidence include a number of sources which are fainter than this limit (sources not disturbed by glitch residuals or memory effects and seen in overlapping frames).

3. Results

The spatial distribution of all of the detected point sources is displayed in Fig. 1, where we also indicate the extent of the cloud core as represented by the visual extinction (Cambrésy 1999). Unfortunately it was necessary to avoid the densest part of the cloud because it contains sources which would saturate the detector. From the colour/magnitude diagram (Fig. 2) we have separated out the reddest sources and it is clear that the spatial distribution of these correlates well with the visual extinction. Some of these stars are known to be YSOs, but interstellar reddening, if present in the $m_{6.7}$–$m_{14.3}$ colour index, could at least partly explain the spatial distribution of the 'red' sources. However, it would then be hard to explain why we also observe (background) sources with normal colour indices in the most obscured regions. For stars observed in the near-IR (as detailed below) we can clarify the situation; in Fig. 3 we plot H–K versus K–$m_{6.7}$ and we see both the effect of interstellar reddening and intrinsic mid-IR excess (in this case at 6.7 μm). Thus, background stars, which should have colour indices close to zero, scatter along a reddening line. This line may differ between different clouds and has not yet been accurately determined, but we see that the reddening as tentatively determined for two other clouds, agrees well with the trend in the present data. The sources with red $m_{6.7}$–$m_{14.3}$ colours are all, with only two exceptions, located to the red side of the reddening band, confirming the intrinsic mid-IR excesses. We also note that two sources, ISO-CrA-135 and ISO-CrA-140, not detected in the 14.3 μm filter are located in the region of sources with intrinsic mid-IR excesses. These two sources are added to our list of sources with mid-IR excesses (Tab. 1). A third source, ISO-CrA-149, is a less clear case and it is not included in the list.

One of the two sources that lack excess emission at 6.7 μm, ISO-CrA-110, is identical to HR7169, one of the two bright B8V stars in the foreground of the cloud. These stars are associated with bright refection nebulosity, and their Strömgren indices (including Hβ) indicate that they are young (Westin 1985). It is interesting to note that one of these stars have circumstellar material left (probably

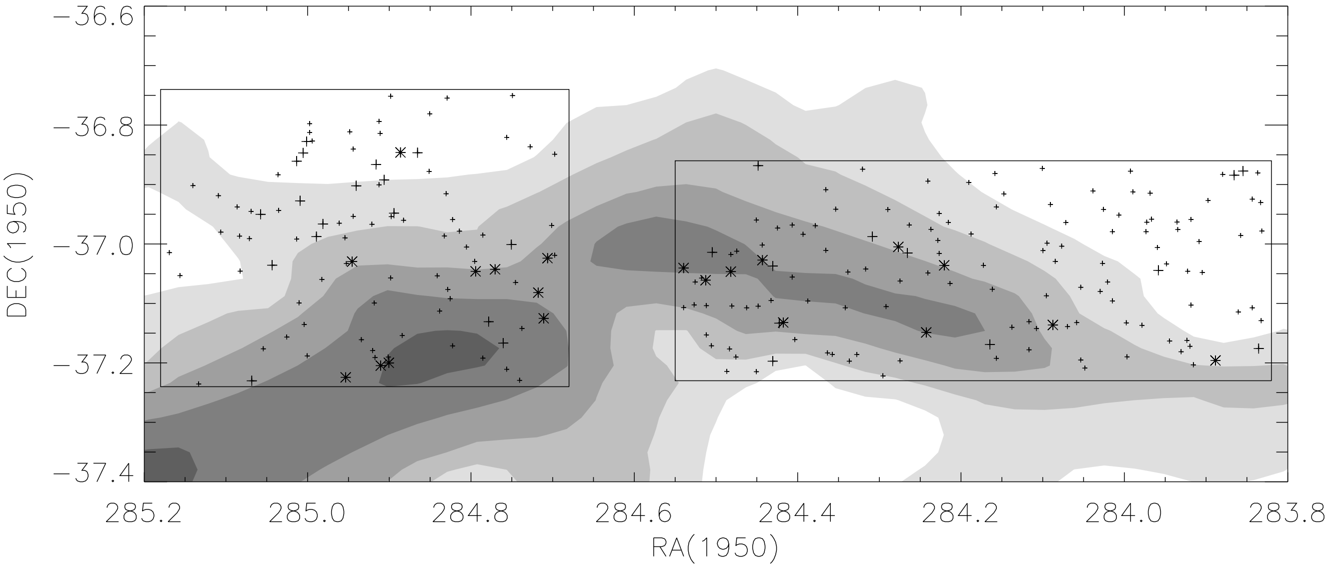

Fig. 1. The spatial distribution of the ISOCAM detected sources, where the asterisks and the large plus signs represent 'red' and 'blue' sources respectively in the $m_{6.7}$–$m_{14.3}$ colour index. The small plus signs represent sources only detected at $6.7\,\mu$m. The contours represent the visual extinction in magnitude steps (Cambrésy 1999).

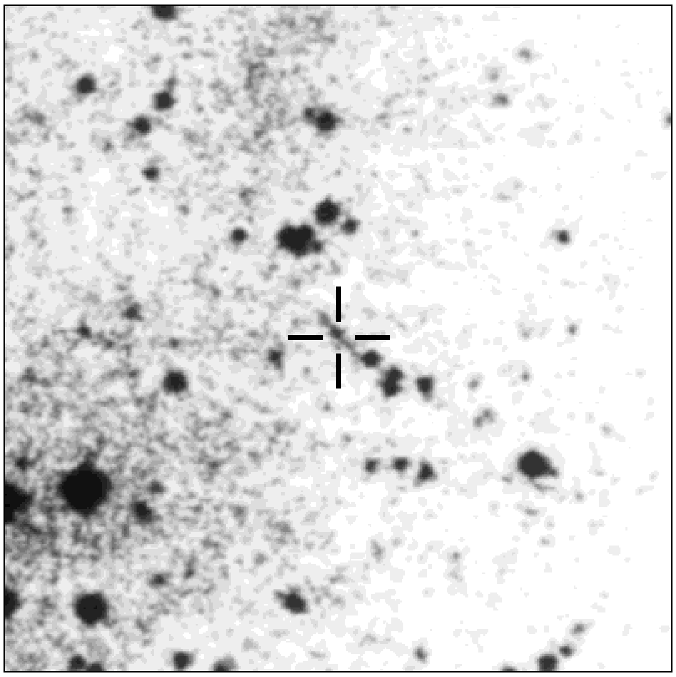

Fig. 4. On this high contrast reproduction of the ESO-J film a faint elongated structure is visible at the position of ISO-CrA-83

disc-shaped) while the other has not. The fact that there is no excess emission at $6.7\,\mu$m suggests that any dust close to the star has vanished. This star should be further studied at a higher spatial resolution from the ground. It should also be noted that at least one of these stars is an X-ray source (Patten 1998).
The other source which has excess emission at $14.3\,\mu$m but not at $6.7\,\mu$m, ISO-CrA-88, is identical to an X-ray source, R9 in Patten's list.

In Tab. 1 we list all the sources which show mid-IR excesses and which are therefore YSO candidates. We include cross-correlations to other observations, but before we turn to the discussion, it is of interest to check whether there are other YSOs (or YSO candidates) previously found within the ISOCAM fields for which we lack evidence for mid-IR excess. Only five such sources (Tab. 2) have been identified and one of them is the previously mentioned B8V star HR7170. All of the others are X-ray sources. For two of them we cannot exclude the presence of mid-IR excess as we lack LW3 detections. For one of the remaining two X-ray sources, ISO-CrA-151, YSO status has been independently confirmed (CrAPMS3 in the investigation by Walter et al. 1997).

4. Discussion

For 21 sources in Tab. 1 there were previous indications of early evolutionary characteristics (X-ray, line emission, Li absorption and/or IR excess) for 7 objects (ISO-CrA-88, 110, 116, 135, 155, 159 and 182). As many as 15 of the sources are visible on the ESO R and J survey, most of them faint. We have applied the method and calibrations described by Hörtnagel et al. (1992) to estimate the magnitudes of the detected sources (except the brightest ones). In Tab. 3 we list these estimates. One of the sources, ISO-CrA-83, appears on both the plates as a very faint,

Table 1. ISOCAM sources with mid-IR excesses.

ISO-CrA	RA(1950)	DEC(1950)	F(6.7), Jy	F(14.3), Jy	F(14.3)/F(6.7)	Source id.
13	18:55:33.2	-37:11:45	0.144	0.065	0.45	
55	18:56:21.0	-37:08:10	0.0040	0.0052	1.30	
76	18:56:52.9	-37:02:09	0.0032	0.0058	1.81	
83	18:56:58.2	-37:08:55	0.0106	0.0145	1.37	
88	18:57:06.4	-37:00:17	0.0176	0.0081	0.46	GPg2, R9
110	18:57:40.2	-37:07:55	0.184	0.161	0.88	HR 7169, R5
116	18:57:46.4	-37:01:37	4.66	6.15	1.32	SCrA, VSS3, R8
127	18:57:55.6	-37:02:47	0.031	0.030	0.98	
134	18:58:03.0	-37:03:39	0.139	0.077	0.55	VSS18, W97-2-2
135	18:58:04.2	-37:03:26	0.0149			Gpe2, W97-2-3, R7
139	18:58:09.5	-37:02:25	0.0106	0.0040	0.38	IRS14, W97-1-12
140	18:58:47.4	-37:01:08	0.0080			W97-1-79
143	18:58:50.6	-37:07:30	0.0041	0.0046	1.12	W97-1-83
145	18:58:52.2	-37:04:54	0.0112	0.0092	0.82	W97-1-89
155	18:59:04.9	-37:02:33	0.167	0.139	0.83	Hα14, W97-2-24
159	18:59:10.6	-37:02:45	0.233	0.181	0.77	Hα3
177	18:59:32.7	-36:50:45	0.0107	0.0073	0.68	
182	18:59:36.1	-37:11:59	0.0249	0.106	4.27	iras32c
185	18:59:38.5	-37:12:16	0.0148	0.0121	0.82	iras32d
198	18:59:46.9	-37:01:46	0.062	0.034	0.55	
201	18:59:48.8	-37:13:27	0.0060	0.008	1.33	

Notes to the table: GP denotes sources observed by Glass & Penston (1975)
VSS denotes sources observed by Vrba, Strom & Strom (1976)
R denotes sources observed by Patten (1998)
IRS denotes sources observed by Taylor & Storey (1984)
Hα denotes sources observed by Marraco & Rydgren (1981)
W97-1- and W97-2- denotes sources in table 1 and table 2 respectively in Wilking et al. (1997)
iras denotes sources in Wilking et al. (1992)

Table 2. YSOs without detected mid-IR excesses.

ISO-CrA	RA(1950)	DEC(1950)	F(6.7), Jy	F(14.3), Jy	F(14.3)/F(6.7)	Source id.
46	18:56:09.2	-36:54:38	0.0147			R13(?)
94	18:57:16.9	-36:52:27	0.0092			R14
111	18:57:41.4	-37:07:59	0.2215	0.0594	0.27	HR 7170
118	18:57:47.6	-36:52:05	0.0364	0.0063	0.17	GPf2, R15
151	18:59:00.1	-37:00:03	0.0266	0.0065	0.24	GPw, R10, W97-99

elongated source with a possible enhancement in the middle, see Fig. 4. It could be a YSO with two jets or possibly an edge-on galaxy. Clearly, this object should be further studied to reveal its nature. The possible inclusion of a galaxy in this list of YSO candidates raises the question of 'contamination' of our sample by background sources. We have used the model of the mid-IR point source distribution developed by Wainscoat et al. (1992) and statistically there should be no AGB or M7III star (which have mid-IR SEDs similar to those of YSOs) in our field. There could, however, be a few galaxies among our sources as indicated by the galaxy counts in Rowan-Robinson et al. (1999) based on deep ISOCAM observations. We have recognised one possible galaxy in our sample, and we cannot exclude that there are additional ones, even though the spatial correlation of the mid-IR excess sources to the dust cloud (Fig. 1) remains a good argument for the YSO assumption.

The main purpose of this ISOCAM survey of nearby star formation regions is to shed light on the IMF for low-mass stars. To determine the mass of a given YSO we need the total luminosity, the age (or effective temperature) and a theoretical model for the PMS evolution. Clearly we lack detailed information for most of the sources in the sample. The most direct method to derive the total luminosity is simply to integrate over the SEDs, including the far IR (see e.g. Wilking et al. 1992), which requires a broad spectral coverage. Another method is to

Table 3. ISOCAM 'red' sources with optical counterparts.

ISO-CrA	m_{ESO-J}	m_{ESO-R}
13	17.7	14.1
55	20.5	17.5
88	16.1	14.1
127	21.1	18.1
134	20.8	17.2
135	16.8	12.5
143	21.1	18.0
155	14.6	11.5
159	17.4	14.1
177	18.9	16.6
198	21.1	17.2
201	19.9	16.4

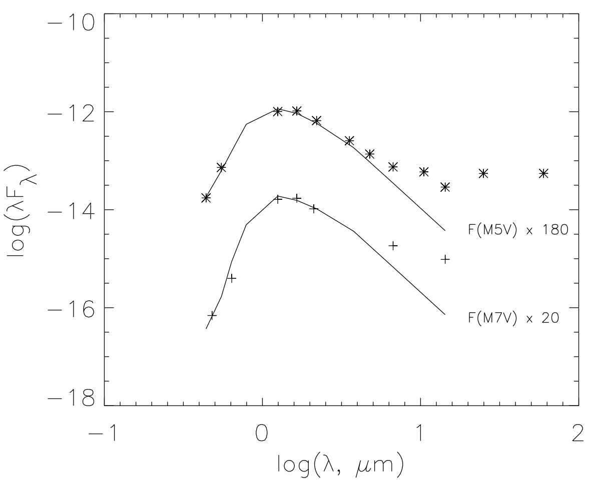

Fig. 5. The SEDs for two 'red' sources with no (or little) interstellar extinction, ISO-CrA-155 (upper) and ISO-CrA-143 (lower) compared to scaled SEDs for M dwarfs.

assume (either by a knowledge of the spectral type or by making *ad hoc* assumptions) an intrinsic near-IR colour and to correct for the interstellar reddening. Finally an empirical relation between e.g. the J luminosity and the total luminosity is used (see e.g. Greene et al. 1994). In the following we will adopt the latter method, but since we lack J observations for most of our sources we instead use the observed luminosities at 6.7 μm. This approach assumes that the dust emission at 6.7 μm scales to the photometric flux at shorter wavelengths, which might be the case if the dust emission mainly is due to re-processed light from the photosphere. We thus expect that it may work for sources that have passed their main accretion phases but probably not for younger sources, for which the bulk of the emission escapes in the far IR. It should obviously not work for YSOs that no longer have any circumstellar dust. The advantage of using the 6.7 μm instead of the J luminosity is the much lower extinction

Table 4. Derived properties for ISOCAM sources with known spectral classes and small interstellar extinction. The age and mass estimates are based on model calculations by D'Antona & Mazzitelli (1998).

ISO-CrA	$\log(L/L_\odot)$	$\log(T_{\rm eff})$	age, years	$M/M_\odot$
88	-0.71	3.52	1e6	0.18
116	0.74	3.64	7e4	0.55
135	-0.93	3.52	2e6	0.22
143	-1.95	3.42	5e5	0.03
155	-0.14	3.52	7e4	0.18
159	-0.35	3.52	2e5	0.20

correction required at 6.7 μm. To proceed along this line, we first need a calibration of the relation between the 6.7 μm luminosity and the total luminosity, and to this end we start by looking closer at our sample of YSO candidates:

With the exception of the two extreme cases, the B8V star HR7169 which has escaped the cloud and has a SED peaking in the blue and the Class I source IRAS 32c which has a rising SED in the mid-IR (Wilking et al. 1992), the intrinsic SEDs of the sources are probably dominated by late type photospheres. To illustrate this, we first select two sources which seem to be little effected by extinction (from their H–K colours), ISO-CrA-143 and 155, and which span a relatively wide luminosity range and we note a striking similarity (Fig. 5). The spectral class for ISO-CrA-155 has been estimated by Patten (1998) as M5V/M3IIIe and as a comparison to the observed SED we use the SED for a M5.5 dwarf as given by Leggett (1992). The other source, ISO-CrA-143, has a SED which closely mimics that of an M7 dwarf. Such late dwarfs at a distance of 129 pc would appear much fainter but if we scale their SEDs to the levels of the YSOs we find that the agreement is good in the optical/near-IR and that these YSOs have mid-IR excesses, which extend into the far IR for at least the brighter source. However, the IR excesses add very little to the integrated fluxes. Three additional sources in our sample with small interstellar extinction, ISO-CrA-88, 135 and 159 also have spectral classes (in fact the same as for ISO-CrA-155) determined by Patten (1998) and assuming an intrinsic colour index V–I_C = 2.7 he also estimated the visual extinction. We apply extinction corrections and integrate the fluxes for these sources as well. The effective temperature that corresponds to the cited colour index is 3300 K (Leggett et al. 1996). If we in addition include ISO-CrA-116 (SCrA) with a luminosity determined by Wilking et al. (1992) and an (uncertain) K5 photospheric spectrum we have effective temperatures and luminosities for six sources (Tab. 4).

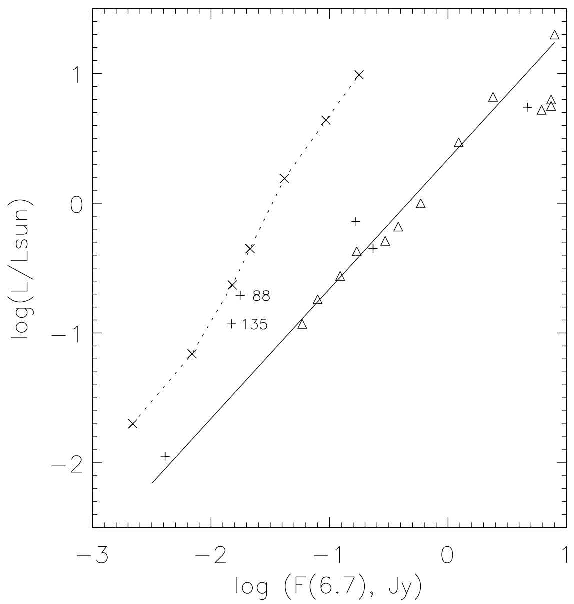

Fig. 6. For the six CrA sources in Tab. 4 (+) and a number of ChaI YSOs (triangles), the monochromatic flux at 6.7 μm scales relatively well with the integrated luminosity (the full drawn line is a linear fit with an imposed slope = 1). The dashed line represents the approximate locus for *bare* stars at an age of 1 million years, where we have used the evolutionary models by D'Antona & Mazzitelli (1998). The crosses represent the following masses: 0.05, 0.1, 0.2, 0.4, 0.8, 1.6 and 2.5 in solar units.

In Fig. 6 we plot the derived luminosities versus the fluxes at 6.7 μm. We also include a similar sample of YSOs in the ChaI region, scaled to the same distance as the RCrA region (Olofsson et al. 1999). The relatively tight relation means that the dust emission at 6.7 μm is roughly proportional to the total luminosity and we can use this relation to estimate the luminosities for all the other sources in our sample of mid-IR excess sources. In Fig. 6 we also include the locus of *bare* YSOs at an age of one million years. As expected, the sources ISO-CrA-88 and ISO-CrA-135, for which we found no and modest colour excesses in the index K − $m_{6.7}$ (see Fig. 3), are located close to this relation for bare YSOs. This illustrates that intrinsic individual differences between the sources give rise to a scatter in the relation. For an interpretation of this scatter, see Bontemps et al. (1999).

Before we use this relation for the remaining sources to estimate luminosities, we must consider an obvious problem: the sources in Fig. 6 suffer from little or no extinction at 6.7 μm which is not necessarily true for the other sources. But as mentioned previously, 15 of the 21 sources are seen on the ESO J plates, and for these sources the extinction at 6.7 μm has to be small. For those sources with near-IR observations, we can correct for the interstellar extinction; the intrinsic H–K colour index remains relatively constant for late-type stars (0.3–0.5) and if we neglect the possible intrinsic colour excess, we can estimate the reddening. In the particular case of the RCrA region, Wilking et al. (1997) derived a reddening different from that of the diffuse medium: $E_{J-H}/E_{H-K} = 1.5$. Assuming that the extinction in the near-IR can be described by a power law, $A_\lambda \propto \lambda^{-\beta}$, the corresponding exponent is $\beta = 1.47$. If we in addition assume (as is usually done) that the absolute extinction at K can be estimated by extrapolating to infinite wavelength, we get the relation $A_K = 1.89\ E_{H-K}$. For the extinction at 6.7 μm we cannot use this power law, as there are absorption bands within the filter pass-band, but as $E_{K-m_{6.7}} \approx E_{H-K}$ (see Fig. 2), we find that $A_{6.7}= 0.47\,A_K = 0.9\,E_{H-K}$. This is by itself a remarkable result (much higher extinction in the 5.5–8 μm region than expected), but it agrees with the result presented by Lutz et al. (1996).

Thus, for the sources with published observations in H and K we estimate the extinction at 6.7 μm (assuming the intrinsic colour index H–K = 0.4), correct the observed LW2 flux accordingly and use the relation $\log(L/L_\odot) = \log(F(6.7,Jy))+0.34$ (see Fig. 6) to derive the luminosity. For two sources, ISO-CrA-76 and 185, which are invisible in the optical, we lack information in the near-IR and consequently the estimated luminosities remain uncertain. For the Class I source, IRAS32c = ISO-CrA-182 we use the bolometric luminosity given by Wilking et al. (1992) and for HR7169 we can directly assign a mass from its spectral class, B8V.

As our main goal is to estimate the mass distribution, we now need a relation between the luminosity and the mass. The luminosity for PMS stars is a function of age and the problem is of course that we lack enough information to assign individual ages. For the six sources in Tab. 4 we have age estimates from $7\,10^4$ to $2\,10^6$ years and Patten (1998) find a similar range of ages for the emission line objects in the region. We use the mass/luminosity relations for 0.5, 1, and 2 million years from D'Antona & Mazzitelli (1998) to derive the mass distribution and the result is shown in Fig. 7. It should be noted that we have not attempted to correct for double stars, which means that the number of sources in lowest mass bins should be corrected upwords. In addition, the completeness limit of the survey roughly corresponds to $0.1\,M_\odot$. For these reasons, and because of the relatively small number of sources, no firm conclusion about the IMF below $0.1\,M_\odot$ can be drawn.

5. Conclusions

Based on an ISOCAM survey of the RCrA star formation region we have found 21 sources with intrinsic excess emission in the mid-IR and therefore identified as YSO

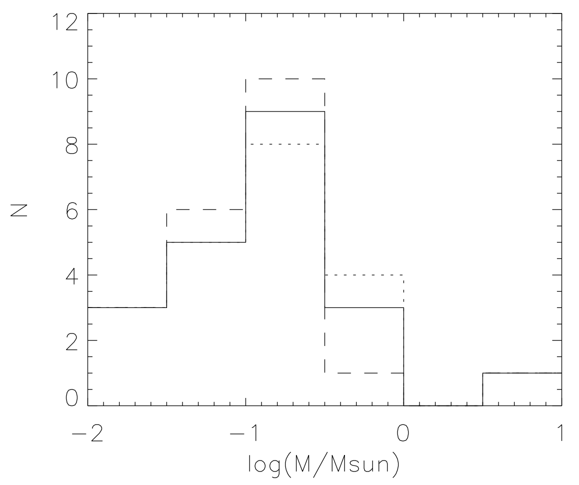

Fig. 7. The distribution of stellar masses for the YSOs with mid-IR excess emission. The masses, except for the six sources in Tab. 4, were calculated assuming co-eval star formation 0.5 (dashed line), 1 (full drawn line) and 2 (dotted line) million years ago. Note that no correction has been applied for possible double stars, and that the completion limit of the survey roughly corresponds to 0.1 M⊙.

candidates. Only 7 of these source have been noticed before as YSOs. Although spectroscopic information is required for each source to confirm its membership of the young population, we argue that the 'contamination' of background sources should be small, and using a few, relatively simple steps we have estimated the masses for the YSO candidates. Due to the small number of sources, no firm conclusion on the IMF can be made, but it is interesting to note that one third of the sources is below the brown dwarf limit (0.08 $M_{\odot}$). Two of these are, however, quite uncertain due to unknown extinction and a third source (ISO-CrA-83) may actually be a galaxy. Clearly these sources should be further studied from the ground. One unfortunate circumstance concerning these ISOCAM observations was the imposed gap in the map at the most active part of the cloud. It should be realised, however, that sensitive mapping from the ground in L′ (3.7 μm) in combination with the already existing sensitive JHK′ maps by Wilking et al. (1997) should be efficient in identifying sources with intrinsic mid-IR excesses. Such observations are being planned.

Acknowledgements. The Swedish participation in this research is funded by the Swedish National Space Board

References

Anderson, I.M., Harju, J., Knee L.B.G. Haikala, L.K. 1997, A&A 321,575

Bontemps S., Nordh L., Olofsson G., et al. 1999, to be submitted to A&A

Bontemps, S., Nordh, L., Olofsson, G. , Huldtgren, M., Kaas, A.,A., Andre, P., Cesarsky, C., J., Montmerle, T., Abergel, A., Boulanger, F., Cesarsky, D., Lagache, G., Puget, J. L., Blommaert, L., Burgdorf, M., Prusti, T., Copet, E., Davies, J., Falgarone, E., Perault, M., Persi, P., Sibille, F. 1998, in: *Star Formation with the Infrared Space Observatory (ISO)*, Eds. J.L. Yun and R. Liseau, p. 141

Brown, A. 1987, ApJ 322, L31

Cambrésy, L. 1999, A&A *in press*

D'Antona, F., Mazzitelli, I. 1998, model calculations made available on th web site http://www.sporzio.astro.it/~dantona/prems.html and described in: *Cool Stars in Clusters and Associations*, Eds. R. Pallavicini and G. Micela, Mem.S.A.It. 68, 807

Glass, I.S., Penston, M.V. 1975, MNRAS 172, 227

Graham, J.A. 1991, in: *Low mass Star Formation in Southern Molecular Clouds,* Ed. B. Reipurth, ESO Sc. Rep. 11, 185

Greene, T.P., Wilking, B.A., André, P., Young, E.T., Lada, C.J. 1994, ApJ 434, 614

Harju, J., Haikala, L.K., Mattila, K., Mauersberger, R., Booth, R.S., Nordh, L. 1993, A&A 278, 569

Hartigan, P., Graham, J.A. 1987, AJ 93, 913

Hörtnagel A.M., Kimeswenger S., Weinberger R. 1992, A&A 262, 369

Kaas, A.A. 1999, AJ 118, 558

Kaas A.A., Olofsson G., Bontemps S., et al. 1999, to be submitted to A&A

Kenyon S.J., Hartmann L. 1995, ApJS 101, 117

Leggett, S.K., 1992 ApJS 82, 351

Leggett, S.K., Allard, F., Berriman, G., Dahn, C.C., Hauschildt, P.H. 1996, ApJS 104, 117

Lutz, D., Feuchtgruber, H., Genzel, R. et al. 1996, A&A 315, L269

Marraco, H.G., Rydgren, A.E. 1981, AJ 86, 62

Nordh, L., Olofsson, G., Abergel, A. et al. 1996, A&A 315, L185

Nordh, L., Olofsson, G. , Bontemps, S., Huldtgren, M., Kaas, A.,A., Andre, P., Cesarsky, C., J., Montmerle, T., Abergel, A., Boulanger, F., Cesarsky, D., Lagache, G., Puget, J. L., Blommaert, L., Burgdorf, M., Prusti, T., Copet, E., Davies, J., Falgarone, E., Perault, M., Persi, P., Sibille, F. 1998, In: *Star Formation with the Infrared Space Observatory (ISO)*, Eds. J.L. Yun and R. Liseau, p. 127

Olofsson, G., Kaas, A.A., Bontemps, S. et al. 1999, In:*The Universe as seen by ISO*, Eds P. Cox and M.F. Kessler, ESA SP-427, 459

Ott, S., Abergel, A., Altieri, B. et al. 1997, In:*Astronomical Data Analysis Software and Systems*, Eds. G. Hunt and H.E. Payne, ASP Conf. Ser. 125, 34

Patten, B.M. 1998, ASP Conf. Ser. 154, *The Tenth Cambridge Workshop on Cool Stars, Stellar Systems and the Sun*, Eds. R.A. Donahue and J.A. Bookbinder, p.1755

Rowan-Robinson, M., Oliver, S., Efstathiou, A. et al. 1999, In:*The Universe as seen by ISO*, Eds P. Cox M.F. Kessler, ESA SP-427, 1011

Starck, J.L., Abergel, A., Aussel, H., Sauvage, M., Gastaud, R., Claret, A., Desert, X., Delattre, C., Pantin, E. 1999, A&AS 134, 135

Taylor, K.N.R., Storey, J.W.V. 1984, MNRAS 209, 5P

Vrba, F.J., Strom, S.E., Strom, K.M. 1976, AJ 81, 317

Wainscoat, R.J., Cohen, M., Volk, K., Walker, H.J., Schwartz, D.E. 1992, ApJS 83, 111

Walter, F.M., Vrba, F.J., Wolk, S.J., Mathieu, R.D., Neuhäuser, R. 1997, AJ 114, 1544
Westin, T.N.G. 1985, A&AS 60, 99
Wilking, B.A., Greene, T.P., Lada, C.J., Meyer, M.R., Young, E.T. 1992, ApJ 397, 520
Wilking, B.A., McCaughrean, M.J., Burton, M.G., Giblin, T., Reyner, J.T., Zinnecker, H. 1997, AJ 114, 2029